Shear-wave velocity based evaluation of liquefaction resistance of calcareous sands of different origin

PORCINO D.D., Tomasello G. (2019). Shear-wave velocity based evaluation of liquefaction resistance of calcareous sands of different origin. S*OIL DYNAMICS AND EARTHQUAKE ENGINEERING*,vol. 122, 233-247, DOI: 10.1016/j.soildyn.2019.03.019

Shear wave velocity-based evaluation of liquefaction resistance for calcareous sands of different origin

Authors: Daniela D. Porcino [(1)] & Giuseppe Tomasello [(2)]

Abstract

This paper presents the results of an experimental research carried out in laboratory aimed at establishing a relationship between cyclic liquefaction resistance (CRR_{field}) and corrected shear wave velocity (V_{S1}) of carbonate sands. Two carbonate skeletal sands, namely Quiou and Dubai, were investigated together with a carbonate non-skeletal sand from Kenya. The programme included also tests on two silica sands prepared and tested in similar conditions for comparison purposes.

The research was based on undrained cyclic simple shear tests and bender element tests in triaxial cell performed on reconstituted specimens of sand at different initial density and stress states. The results obtained highlight that data points for carbonate sands are all located to the right of the currently used cyclic liquefaction resistance vs. shear wave velocity curves suggested for silica sands, implying that the latter curves should be considered non-conservative when applied to carbonate crushable sands.

An insight into the effect of the initial effective vertical stress on liquefaction susceptibility of carbonate sands was presented and a stress normalization procedure was also proposed.

Keywords: carbonate sands, shear wave velocity, liquefaction resistance, correlation, cyclic simple shear tests

(1) *Associate Professor in Geotechnical Engineering, University "Mediterranea" of Reggio Calabria – Dept. DICEAM, Via Graziella (Feo di Vito) 89124 Reggio Calabria (Italy) – email: daniela.porcino@unirc.it*

(2) *PhD Student in Geotechnical Engineering, University "Mediterranea" of Reggio Calabria – Dept. DICEAM, Via Graziella (Feo di Vito) 89124 Reggio Calabria (Italy) – email: giuseppe.tomasello@unirc.it*

1. Introduction

The significance of damage which can be caused by liquefaction in calcareous sediments has been recognized for many years and has been made sorely clear by numerous catastrophic earthquakes such as the Guan earthquake of 1993, the Hawaii earthquake of 2006, the Haiti earthquake of 2010 and others [1]. Due to soil liquefaction, there may be ground subsidence and settlements, sand boils, lateral spreading, slope failures and damage or even collapse of structures.

It is well known that carbonate sands (with skeletal grains) exhibit unconventional different features from those of silica sands, since they have considerably higher angularity, lower grain hardness and higher intraparticle porosity, resulting in high friction angles [2]. Therefore, it is not surprising that there are significant differences in terms of compressibility, volume changes and grain crushing during shearing yielding, friction and water permeation, among various types of calcareous sands with respect to silica sands [3-8]. The behaviour of the oolitic non-skeletal sands is to some extent intermediate between silica and carbonate skeletal sands [9].

Existing procedures for estimating liquefaction potential are currently based on empirical data gathered from sites primarily involving silica sandy soils and a review of the relevant liquefaction literature did not reveal specific procedures for sandy soil having other mineralogy types or origins. The use of shear wave velocity (V_S) offers engineers a promising alternative and supplementary tool to evaluate liquefaction resistance of soils. The advantages of a V_S-based method have been discussed by many researchers (i.e. [10-11]) and guidelines for evaluating liquefaction potential using V_S measurements are presented in Andrus et al. [12]. As pointed out by Seed [13], with field seismic conditions being properly simulated, the controlled laboratory studies could be used to broaden the applicability of liquefaction criteria, especially for the conditions where little to no field performance data is available. The application of laboratory-based approach to field conditions would require a proper consideration of the following aspects:

- adjustment allowing for the different stress states of V_S (laboratory vs. field measurements);
- conversion of the cyclic stress ratio to cause liquefaction for field K_0 conditions;
- effect of two-dimensional shaking in the field;
- evaluation of the equivalent number of uniform stress cycles (N) of earthquake shaking as a function of earthquake magnitude;

- influence of in-situ fabric of soil deposits, in consideration of the fact that laboratory *CRR*-V_S correlations are essentially derived from data of reconstituted specimens.

The concept of such research lies in the fact that soils of the same type, which have the same shear wave velocity under the same stress conditions, would also have the same liquefaction resistance [14]. Examination of the available studies focusing on this subject on clean silica sands [14-18] and silty sands [19-22] suggests the validity of laboratory V_S-based methods and a close agreement between laboratory and field studies for liquefaction assessment. However, extensive research on carbonate sands in this field is lacking (i.e. [23-26]) and additional data are needed to further validate the laboratory-based approach.

This research will directly address this deficiency by developing new relationships between liquefaction resistance and V_S for carbonate sands, based on a comprehensive laboratory investigation. To meet this objective, a total of thirty four undrained constant volume cyclic simple tests to liquefaction and fifteen bender element tests for measuring shear wave velocity, were carried out on reconstituted specimens of three carbonate sands of different origin (skeletal and non skeletal) and two silica sands under the same initial state conditions, for comparison purposes. The influence of mineralogy and crushing features on undrained cyclic characteristics of the tested sands were also presented through test results.

2. Tested materials, test device and testing procedures

Laboratory investigation was performed on three carbonate sands, namely Kenya (*KS*), Dubai (*DS*) and Quiou (*QS*). Fig.1 shows the microscopic pictures of calcareous sand grains tested in the present study. The grain size distribution curves of tested sands are shown in Fig.2, while physical properties and test conditions are reported in Table 1 and Table 2, respectively. Additionally, two silica sands, namely Ticino (*TS*) and Ticino fine (*TSF*), were tested for comparison purposes.

The tested *QS* [9, 29-30] is a biogenic (skeletal) sand dug out from a borrow pit close to the village of Plouasne in Brittany (France). It consists of a greyish white sub-angular uncemented calcitic carbonate coral sand [9] made of 61.2% shell fragments, 14.2% calcium carbonate aggregates, 18.1% quartz and 6.5% rock fragments.

Dubai carbonate sand was recovered at a relatively young biogenic calcareous sand deposit at Dubai site, in the United Arab Emirates (UAE) [31]. It has a carbonate calcium

content equal to 55%. Microscope images evidenced sub-angular grain shape and a high presence of shells or fragments of shells (Fig.1c). Geological and geotechnical characteristics of the Arabian Peninsula, with particular emphasis on the Emirate of Dubai, is also documented in the investigations performed by several authors (i.e. [32-33]).

Kenya sand (*KS*) is a non skeletal (oolitic) carbonate sand with particles made of 97% carbonate, 2% quartz, and 1% feldspar. *KS* is almost uniform, fine, and the sub-rounded particles are less prone to grain crushing [34].

Due to their mineralogical composition, these calcareous sands have higher values of specific gravity (G_s) than those measured for silica sands. The index properties of silica sands used for comparison purposes are also listed in Table 1, while their grain size distribution curves are shown in Fig.2. It is worthwhile mentioning that the two silica sands have different mineralogical features with respect to carbonate sands but similar grain size characteristics and particle size distributions.

Laboratory testing program (Table 2) comprised cyclic undrained simple shear (*CSS*) tests and bender element tests in triaxial cell (*BE*). It is worth mentioning that working with crushable sands, some laboratory test issues arise related to their crushable nature and specific morphology. An in depth discussion of all these aspects is reported in Van Impe et al. [35].

Cyclic simple shear tests were performed by a modified cyclic simple shear *NGI* (Norwegian Geotechnical Institute) apparatus [36]. The specimens are 80 mm in diameter and 20 mm in height, and they are laterally confined by a reinforced rubber membrane, capable of assuring conditions of zero horizontal deformation (K_0 consolidation). Excess pore water pressures during undrained shear are inferred from the change in total stress required to maintain constant volume (i.e. height) conditions. It has been shown that the decrease (or increase) of vertical stress in a constant-volume *SS* test is essentially equal to the increase (or decrease) of pore-water pressure in an undrained *SS* test, where the near-constant-volume condition is maintained by not allowing the mass of pore water to change. The good correspondence between truly undrained and equivalently undrained constant volume tests in simple shear apparatus was experimentally verified under both monotonic and cyclic loading conditions on saturated clays and dry sands [37-38].

Thus, membrane compliance problems which could otherwise affect pore water pressure measurements during undrained tests are avoided in constant volume undrained *SS* tests. It should be mentioned that different reconstitution methods were adopted in the present

study in order to replicate in-situ fabric of natural sand deposits as closely as possible. In case of fine sands, specimen preparation by water sedimentation appears to be very problematic causing appreciable segregation of material.

In the present study, water sedimentation was adopted for sands of marine or fluvial origin (i.e. Ticino, Quiou) while air pluviation was adopted for the calcareous *KS* and *DS* and the silica *TSF* and *TS*. During pluviation, a funnel was displaced back and forth laterally to maintain an approximately levelled surface of the soil. After filling the cavity, the excess sand over the final grade was siphoned off by applying a small vacuum. Samples prepared by the above pluviation method were in the loosest state. When preparing *SS* specimens by water sedimentation method of carbonate *QS* and silica *TS*, the sand was spooned gently into the water layer by layer, until the height was just above the top of the mould. In this way, density index values I_r=35%-40% were initially achieved, regardless of the drop height. When required, higher initial densities were obtained by tapping the base of apparatus while the specimen was confined under a small seating load.

It is worth mentioning that *CSS* tests were stopped when shear strains in single amplitude (γ_{SA}) reached 3.75%, which was assumed as liquefaction "triggering" criterion in all tests as recommended by several authors [39-40]. At this level of shear strain, residual pore water pressure ratios $R_u=\Delta u/\sigma'_{v0}$ were in the range 0.84-0.98, where the lower values were reached by dense specimens or specimens prepared through water-sedimentation method.

Bender element tests in triaxial apparatus were performed on both silica and carbonate sands after the consolidation phase. Triaxial specimens, approximately 70 mm in diameter and 140 mm in height, were saturated and then isotropically consolidated under an effective confining stress increasing gradually in steps. To obtain accurate measurements of shear wave velocity at the end of isotropic consolidation phase, a sinusoidal wave impulse with an appropriate frequency (in the range 5-10 kHz) was adopted for exciting the transmitter element. Travel time was determined by "time domain first arrival method" [18, 41-43] which treats the first zero crossing as the arrival of shear wave (Fig.3). Then the shear wave velocity (V_S) in the specimen can be calculated from the travel time (t) and the known separation (L) between the bender elements (tip-to-tip) as:

$$V_S = L/t \tag{1}$$

All details of the testing program are summarized in Table 2.

3. Test results

3.1 Bender Element tests

An example of variation of V_S with void ratio for several confining stresses, namely 50, 100 and 200 kPa, is shown for carbonate *QS* in Fig.4.

The reported void ratios (e_0) correspond to the final void ratios at the end of the consolidation phase. It is evident that, for specimens prepared at identical void ratios, the shear-wave velocity of Quiou sand is controlled primarily by the effective confining stresses. It is worth noticing that sand specimens were reconstituted by water sedimentation method and it is generally understood that such a method produces stiffer samples than other specimen preparation methods (i.e., dry pluviation) [44].

Previous laboratory investigation (from resonant column and bender element tests) suggested that high values of V_S (G_0) can be expected in calcareous sands when compared to corresponding silica sands [1, 45-46], as shown in Fig.5 for two sands tested in the present research in terms of shear wave velocity ratio $V_{S,calcareous}/V_{S,silica}$. Test results reveal the importance of mineralogy on small strain properties of sands. Additional microstructure effects can lead to even higher in-situ V_S values since cementation and ageing effects tend to increase the measured in-situ values [47].

V_S is a valuable indicator of dynamic properties of soil because of its relationship with small strain shear modulus, G_0, calculated by the following equation:

$$G_0 = \gamma / g \cdot V_S^2 \quad (2)$$

where γ is the total unit weight of the soil and g is the gravity acceleration (9.81 m/s^2).

For cases where direct measurements of shear wave velocity (V_S) are not available, correlations between V_S and penetration resistances measured in *CPT* and *SPT* tests will be used. It was also verified that, when one considers the correlation between small strain shear modulus and cone resistance (q_c), G_0 data obtained in the present study for uncemented carbonate Quiou sand position well, close to the upper bound given in the literature for uncemented, unaged silica sands [48] (Fig.6). The values of q_c for *QS* were based on the interpretation of Static Cone Penetration Tests (*CPT*) in Calibration Chamber (*CC*) conducted in the context of a previous in-depth research [49-50] (see also [51]).

3.2 Cyclic simple shear tests

Typical results gathered from undrained cyclic simple shear tests (*CSS*) for three sands having similar grain size features, namely: Dubai and Kenya (carbonate) and Ticino fine (silica) are reported in Fig.7. In particular, the stress-paths and stress-strain plots are herein depicted. Sand specimens were tested at the same initial state before shearing and subjected to the same value of cyclic stress ratio ($CSR=\tau_{cyc}/\sigma'_{v0}\cong 0.15$). In general, the specimens exhibited a "cyclic liquefaction" failure mode [52] in symmetrical *CSS* tests: failure was caused by a reduction in the cyclic stiffness, leading to excessive cyclic or "swing" displacements. Shear strains accumulated slowly in the beginning; afterwards, the rate of shear strain increment accelerated, as it is also apparent in the *S*-shaped τ–γ curves in Fig.7 (a, b and c). At the onset of liquefaction (i.e. pore water pressure ratio $R_u=\Delta u/\sigma'_{v0}\cong 0.95$), induced cyclic shear strains reached values approximately equal to 3.75% in single amplitude.

Fig.8 presents normalized excess pore pressure ratio (R_u) as a function of the normalized number of cycles for reaching liquefaction (i.e. N/N_f). Fig.8 highlights the different features in terms of excess pore water pressure (*PWP*) generation between calcareous and silica sands. In particular, calcareous sands developed larger excess *PWPs* than silica sands during the earlier stages of cyclic loading phase except for the non skeletal *KS* (Fig.8b). Furthermore, calcareous sands with the exception of non-skeletal *KS* had greater fluctuations of excess *PWP* between loading cycles, which could have been due to particle rearrangement. These findings are consistent with those reported by other authors on calcareous sands [53-55]. Conversely, silica sands had slow, gradual excess *PWP* generation during the initial cyclic loading phase and very small pore pressure fluctuations between loading cycles. Another important difference was that silica sands typically showed a sudden or abrupt increase in excess *PWP* towards the end of the tests, while a more gradual or incremental increase was shown in calcareous sands as they reached liquefaction.

Fig.9 reports the cyclic resistance ratio (*CRR*) against number of stress cycles required to cause liquefaction (N_f), according to the selected failure criterion. For cyclic simple shear tests, *CRR* is defined as the ratio between applied cyclic shear stress on the horizontal plane and effective vertical consolidation stress, as follows: $CRR=\tau_{cyc}/\sigma'_{v0}$. In particular, a comparison of the liquefaction resistance curves for *KS* (carbonate) and *TSF* (silica) tested

at a medium dense state is shown in Fig.9a. A similar comparison is presented in Fig.9b for loose specimens of *QS* (carbonate) and *TS* (silica).

It can be argued from these figures that carbonate sands in general exhibit a higher or at least comparable liquefaction resistance with respect to silica sands, tested under similar relative densities and effective consolidation stresses, as reported also by other researchers [55-56]. It was verified that such differences in the liquefaction potential of carbonate against silica sands are more evident for dense specimens, as it was ascertained by the comparative experimental data of *KS* against *TSF*. These findings are consistent with those reported also by other authors in previous research involving carbonate soils [53, 57]. Increased cyclic strength is likely to be the result of the angular calcareous sand particle shape, which provides more stable interlocking soil fabric resistant to liquefaction [53, 57-60].

The following power equation was used for interpreting *CSS* test results:

$$CSR = A \cdot N_f^{-B} \tag{3}$$

where *B* is the slope of the *CRR* versus *N* line on a log–log plot. The power Eq.(3) was applied to carbonate sands in simple shear tests only in a limited number of studies.

Based on the best-fit value of the data set, the empirical *A* and *B* parameters of Eq.(3) are reported in Table 3**.** Finally, two important aspects characterize the behaviour of carbonate sands during undrained cyclic loading with respect to corresponding silica sands: 1) higher excess pore pressure ratios and larger fluctuations; 2) higher liquefaction resistance at comparable density states.

Various research have been performed in the literature regarding the effect of stress level on liquefaction susceptibility for calcareous soils [55-56, 57, 60-61] and silica sands [62-64]. The effect of σ'_{v0} on *CRR* of cohesionless soils could in fact depend on many factors, such as hardness, shape [65], size distribution [66] of grains and also their packing state. The consideration of these and other factors could explain the differences found in the existing literature concerning the “stress-effect” on the liquefaction resistance of crushable sands.

For silica sands, the overburden correction factor (K_σ) was introduced to account for the variation of a soil's cyclic resistance ratio (C*RR*) as a function of effective consolidation stress: it decreases as effective overburden stress increases. The factor K_σ describes the curvature of the cyclic strength envelope with increasing consolidation stress and this

curvature is dependent on density index and soil type [67]. An updated database of laboratory test results relative to clean silica sands and silty sands is presented by Montgomery et al. [67], where it is suggested that the relationships by Idriss and Boulanger [68] continue to provide a reasonable basis for evaluating liquefaction effects in clean silica sands.

In this context, Fig.10 presents the influence of initial effective vertical stress (σ'_{v0}) on the liquefaction resistance curves of two carbonate sands, namely the skeletal Quiou sand (Fig.10b) and the non skeletal Kenya sand (Fig.10a). There appears to be a clear dependence of *CRR* on effective vertical stress for dense specimens of Kenya sand, with the cyclic strength decreasing as the effective vertical stress increases. On the other hand, examination of Fig.10(b) for the loose Quiou sand, shows a slight increase of cyclic liquefaction resistance with the increase of σ'_{v0} from 100 kPa to 200 kPa. This was the opposite of the expected behaviour for silica sands since, normally, an increase in effective confining stress results in a more contractive behaviour.

This "unusual" behaviour exhibited by Quiou sand was observed also by other authors for various crushable soils. For example, Hyodo et al. [57], based on undrained cyclic triaxial tests, reported a similar response for the loose Dogs Bay carbonate sand and Shirasu volcanic sandy soil. Furthermore, a similar effect was observed by Mirbaha [69], based on cyclic simple shear tests performed on the loose Boler carbonate-silica sand (see also Table 4).

The increase in *CRR* with increasing σ'_{v0} may be attributed to crushing of the particles and their re-arrangement. In a previous research (Porcino et al. [70]), quantification of the breakage through the changes of grading curves after undrained simple shearing identified for this sand an increase in particle breakage with the increase of stress level in the range 50-200 kPa. An appreciable particle crushing in carbonate sands under shearing was indeed presented by many authors even at low stresses (i.e. Coop [71]).

Following the procedure suggested by Finnie at al. [72], in an attempt to normalize the results of all *CSS* tests and represent them on a single contour diagram, the shear stress ratio required to cause liquefaction, *CRR,* can be redefined in the following alternative form:

$$CRR_{ref} = \frac{\tau_{cycl}}{\sigma'_{ref}} \tag{4}$$

The reference effective vertical stress is calculated as:

$$\sigma'_{ref} = P_a \cdot \left(\frac{\sigma'_{vo}}{P_a}\right)^n \quad (5)$$

where P_a is the atmospheric pressure (i.e. 98.1 kPa), σ'_{v0}= vertical effective stress in the same units as P_a, and n is an empirical parameter to be assessed for a given soil.

Based on Eq.(5), it is readily derived that the liquefaction resistance for a given value of in situ vertical stress σ'_{v0}, can be calculated through the equation:

$$CRR_{\sigma'_{v0}} = CRR_{ref} \cdot \left(\sigma'_{vo}/P_a\right)^{n-1} \quad (6)$$

Determination of the best fit exponent n, which appears in Eqs.(5-6), for a given soil was determined by back-analysis of the CRR_{ref} data in the CRR-log(N) plane, assuming the CRR-N curve at σ'_{v0}= 100 kPa as benchmark response curve (i.e. CRR_{ref}). An optimum best fit n value, corresponding to the lowest root mean square error (*RSME*) from the assumed benchmark response curve, was determined when all data at different σ'_{v0} values were included.

In the present study, in the stress range between 50 kPa and 200 kPa, the best fit exponent n of Eq. (6) varies between 0.78 (Kenya sand) and 1.13 (Quiou sand) (Table 4). Experimental data reported in Fig.10 are then re-plotted in Fig.11 after the application of the described normalization method. Apparently, Fig.11 shows that data points (after normalization) are located around a liquefaction resistance curve which is practically unique, regardless of initial effective vertical stress.

Since *CSS* data on carbonate sands at different σ'_{v0} are not so extensive to provide a clear indication of the variability of the parameter n, additional selected published data on carbonate sands from undrained triaxial tests (i.e. Cabo Rojo, Dogs Bay, North Coast sands) and cyclic simple shear tests (i.e. Boler sand) were also analysed in the present study (Table 4). For cyclic triaxial tests p'_0, in lieu of σ'_{v0}, was considered in Eq.(6).

The exponent n was found to range between 0.44 and 1.28 for these carbonate sands, tested at different density indices and confining stresses (i.e. 50 kPa – 600 kPa). It is worth noting that n can be larger or smaller than 1, depending on whether the increase of σ'_{v0} leads to an increase or decrease of cyclic liquefaction resistance, respectively. Thus, n is a function of many factors including grain crushability and angularity, density state, range of overburden pressures, etc, and more definitive conclusions will be reached considering a collection of a larger database on different carbonate sands.

The effect of stress-path imposed in laboratory tests for cyclic liquefaction resistance assessment of carbonate sands was also investigated. Many different laboratory testing apparatus are used to duplicate the stress state generated in situ by earthquakes and more details can be found in Bhatia et al. [73]. In fact, while triaxial testing is the most widely performed cyclic soil testing method, its applicability in fundamental seismic studies is severely hampered by an inherent stress path problem; as a result, simple shear testing method, including direct simple shear and torsional shear, have become the standard tool in more recent fundamental liquefaction studies [38, 74-76].

Figure 12 presents a comparison between the cyclic liquefaction resistance curves gathered by the authors from triaxial tests in a previous research [77] and simple shear tests carried out in the present study on both loose and dense specimens of Quiou carbonate sand. In the triaxial tests, the failure conditions are based on a double amplitude axial strain (ε_{DA}) equal to 5%, basically corresponding to a single-amplitude shear strain equal to 3.75% in *CSS* tests.

The cyclic resistance of carbonate sands subjected to triaxial stress path was found to be higher than that determined under simple shear mode, regardless of void ratio of the sand (loose and dense specimens) (Fig.12). Thus, it is desiderable to perform simple shear tests if possible, taking into account that an accurate estimation of equivalent simple shear or in-situ response from triaxial test results is rather difficult and it is a complex function of several factors [78], including sand mineralogy.

4. Correlation between shear wave velocity and liquefaction resistance of carbonate sands

The influence of crushability features of sand on *CRR*-V_S correlation was investigated by combining: 1) the CRR_{SS} determined using cyclic simple shear tests on sand specimens and 2) estimates of stress-normalized shear wave velocity corresponding to the void ratio at which the cyclic simple shear tests were performed.

Although the shear wave velocity is a small-strain soil property, it can be related to the liquefaction resistance which involves plastic behaviour. This is because the pore-pressure generation leading to liquefaction is governed by the volume change characteristics of soil at small cyclic shear strain. Besides, the volume change characteristics are governed by the soil fabric and density and so is the small strain shear modulus [14].

CRR_{SS} and V_S data from laboratory testing were converted to in-situ conditions and a direct comparison with field based correlations developed for uncemented silica sands by Andrus & Stokoe [10] and Kayen et al. [79] was made.

It is common practice to convert CRR_{SS} to field conditions through the following expression [13]:

$$CRR_{field} = r_c \cdot CRR_{SS} \tag{7}$$

where CRR_{SS} value is corrected by r_c constant accounting for the effect of multidirectional shaking (r_c in the range from 0.90 to 1.0). A value of r_c = 0.95 was assumed in the analysis of test results in the present study. It is worth noting in Eq.(7) that no field K_0 correction was applied to the results of cyclic simple shear tests.

On the other hand, the laboratory V_S values measured in bender element tests require adjustment allowing for the different stress state. They can be readily converted to:

$$V_{S,field} = V_S \cdot \left(\frac{1 + 2 \cdot K_0}{3}\right)^m \tag{8}$$

where $V_{S,field}$ is the equivalent field value of laboratory V_S at the depth in question, K_0 is the coefficient at rest of in-situ soils and m is a stress exponent.

K_0 values were assumed in the range 0.39-0.43 for the tested sands. However, the effect of in-situ K_0 involved in Eq.(8) on the resulting expression for the equivalent field $CRR–V_{S1}$ relationship could be considered negligible for practical purposes, as suggested also by other authors [18]; furthermore, the values of the exponent m, which is generally assumed close to 0.25 for silica sands (*TS* and *TSF*), was calculated on the basis of the variation of V_S with effective confining stress from bender element tests. For carbonate sands m values were found to be equal to 0.21 (*DS*), 0.25 (*QS*) and 0.34 (*KS*).

Field-based CRR-V_S relationship curves of clean silica sands are generally reported in terms of overburden stress-corrected shear wave velocity V_{S1}, which is calculated according to the following expression:

$$V_{S1,field} = V_{S,field} \cdot \left(\frac{P_a}{\sigma'_v}\right)^{0.25} \tag{9}$$

where V_{S1} is the overburden stress-corrected shear wave velocity, σ'_{v0} is the effective overburden stress (kPa), and P_a is the atmospheric pressure (i.e. 98.1 kPa).

Following the described procedure, all the (CRR_{SS},V_S) data at N=15 cycles were converted into (CRR_{field},$V_{S1,field}$) at the earthquake magnitude M_w=7.5 and plotted in Fig.13a, according to Eqs. 7 and 9.

It is a common practice to assign a value of 15 as equivalent number of cycles for a M_w=7.5, based on the recommendation of Idriss & Boulanger [68]. According to Liu et al. [80], $N_{M=7.5}$ ranges from 19 to 30, depending on the magnitude, epicentral distance, near fault directivity, and site effects.

The comparison between data obtained from laboratory on carbonate sands and field-based liquefaction curves for clean silica sands [10] (Fig.13a) evidences that these data fall to the right of the field-based curves. On the other hand, a quite good correspondence between the results obtained by the two approaches (laboratory/field) for silica sands (*TS* and *TSF*) was found.

The results obtained in the present study support the evidence that, for carbonate soils, the use of the field-based *CRR*-V_S curves adopted for silica sands is non conservative (the liquefaction resistance of carbonate sands is lower than that suggested by the field-based approach), consistently with the recent findings reported in the limited literature for calcareous sands [23-24]. Taken into account the moderate differences in *CRR* values exhibited by calcareous versus silica sands (Fig.9) at equal density state, these findings should be mainly attributed to the higher V_S values of calcareous sands generally reported in the literature and also in the present study (Fig.5).

The procedure proposed by Andrus & Stokoe [10] (deterministic) is based on field performance data from 26 earthquakes and in situ V_S measurements from more than 70 sites in soils ranging from fine sands to sandy gravels with cobbles. The boundary curve by Andrus & Stokoe [10] is plotted in Fig.13a together with the probabilistic curves (dashed curves) corresponding to different liquefaction probability (P_L) (P_L=5%, 15% and 50%), recently developed by Kayen et al. [79]. As can be seen, data points relative to carbonate sands are located to the right of the lowest probability curve at P_L=5% especially in the range of high V_{S1} (>185 m/sec). The consideration of other *CRR*-V_S relationships proposed in the literature (i.e. [18, 21, 81]) would take to the same finding, i.e. the correlations for silica sands provides an unconservative evaluation of the liquefaction resistance of carbonate sands.

With the intent of incorporating the effect of overburden effective pressure on cyclic liquefaction resistance of sands, the normalization procedure described in section 3.2 was

taken into account in the calculation of CRR_{field} values (ordinate of CRR-V_{S1} plot) (Fig.11). For this purpose, the same data points reported in Fig.13a were re-plotted in Fig.13b after the normalization of *CRR*, expressed by Eq.(5). It is apparent that such a normalization procedure to σ'_{ref} tracks the effects of σ'_v on *CRR* for carbonate crushable sands and represents a reasonable adaptation of current practice introducing a K_σ correction factor for high overburden stress in silica sands [82].

The authors recognize that additional data should be collected to allow a more definitive evaluation of the liquefaction resistance of carbonate sands through shear wave velocity. Furthermore, it is worth noticing that the CRR-V_S correlation gathered in the present study from laboratory studies on carbonate sands is expected to be valid only for uncemented freshly deposited soils with little or no "microstructure" effects caused by cementation or ageing.

5. Comparison with other *CRR* field-based correlations for predicting undrained cyclic strength of carbonate sands

With the intent of validating the laboratory-based method relating liquefaction resistance of carbonate sands to shear wave velocity, the CRR_{field} data obtained in the present study on silica *TS* and carbonate *QS* specimens prepared by *WS* reconstitution method, were compared with field-based liquefaction boundary curves based on cone penetration tests previously published by the authors.

Based on the above mentioned considerations, it has been deemed useful to use static Cone Penetration Tests (*CPT*) in Calibration Chamber (*CC*) and undrained cyclic simple shear tests to seek appropriate correlations for predicting undrained cyclic strength of sands. Cone penetration measurements in *CC* were performed in the context of a previous research [51]. Calibration chamber is specially designed to perform tests under strictly controlled boundary conditions both in terms of stresses and strains. As for the normalization of *CPT* tip resistance, the following expression was used [11, 39]:

$$q_{c,1} = C_q \cdot q_c \tag{10}$$

$$C_q = \left(\frac{P_a}{\sigma'_v}\right)^a \tag{11}$$

where: C_q is a normalizing factor for cone penetration resistance and P_a is in the same units used for σ'_{v0} (i.e. 98.1 kPa). The exponent *a* of the normalization factor is assumed to

be constant for both *TS* (*a*=0.55) and *QS* (*a*=0.65) [51], although *a* is strictly dependent on density index (I_r). Truly normalized (i.e. dimensionless) cone penetration resistance can be evaluated by the expression:

$$q_{c,1N} = \frac{q_{c,1}}{P_a} \tag{12}$$

Fig.14 evidences that the correlation between CRR_{field} developed by laboratory *CSS* tests and normalized *CPT* tip resistance ($q_{c1,N}$) measured in the *CC* tests for the silica *TS*, corresponds well to the recommended field-performance-based correlation revised by Idriss & Boulanger [83]. In the same figure, the earlier correlation proposed by the NCEER [84] Working Group for clean silica sands is also presented.

Based on the comparison with the two above correlations, it appears that for clean silica sands at *CRR* values less than 0.14, data points in Fig.14 are in good agreement with the correlation developed by NCEER [84]; however, at higher values of *CRR*, the data points of *TS* match better the correlation suggested by Idriss & Boulanger [83]. It is noteworthy that the correlation proposed by NCEER [84] is slightly unconservative for silica sands especially when dealing with high *CRR* values, as evidenced by Seed et al. [39].

This satisfactory agreement between laboratory vs. field based approaches for silica sands creates the opportunity to extend laboratory-based approach to study other materials, such as carbonate sands in order to investigate the influence of mineralogy, where little to no field performance data are available.

In this context, examination of Fig.14 reveals that data points relative to calcareous Quiou sand fall to the left of the *CPT*-field based curves for clean silica sands, so that the use of these curves appears to provide a slightly conservative estimation of the liquefaction resistance of calcareous sands.

The opposite trend exhibited by calcareous sands against silica sands depending on whether their liquefaction susceptibility is evaluated by correlations with *CPT* (Fig. 14) or V_S (Fig.13a) is justified by the fact that, at comparable values of void ratio and stress level, the penetration resistances (q_c) in carbonate sands is lower than in silica sands. This is because the cone penetration causes a greater particle breakage around the tip of the probe in carbonate sands. Conversely, shear wave velocities (V_S) in carbonate sands are generally higher than in silica sands. This makes the *CRR*-q_c correlation of calcareous

sands to lie on the left side of the corresponding field-based curves of silica sands whereas *CRR*-V_S correlation of calcareous sands is shifted to the right.

Despite the "unusual" geotechnical features of calcareous sediments (random and generally weak to moderate cementation, angularity of grains, high void ratios and grain crushing) the behaviour of calcareous sands is consistent with mean features of critical state soil mechanic [5, 85]. For this reason, following a critical state framework, the results of cyclic simple shear tests performed on the calcareous *QS* and *KS* together with the silica *TS*, were also examined in terms of the relative state parameter index (ξ_R) proposed by Boulanger [82, 86].

Several authors adopted a state parameter-based approach to clean silica sands for the analyses of cyclic triaxial test results, for which an accurate estimation of the reference line of sand (steady state/critical state line) from laboratory tests is required.

Following the procedure suggested by Bolton [87], the relative state parameter index (ξ_R) is herein defined as the difference between the current I_r and the critical state I_r, denoted $I_{r,cs}$, by an expression based on Bolton's [87] relationship:

$$\xi_R = I_{r,cs} - I_r = \frac{1}{Q - \ln\left(\frac{100 \cdot p'}{P_a}\right)} - I_r \qquad (13)$$

where p' is the mean effective stress, equal to $\sigma'_{v0} \cdot (1+2K_0)/3$ and K_0 corresponds to the earth pressure coefficient at rest, whose values were assumed according to considerations reported in the previous section 4.0.

I_r is expressed by fraction of unit and P_a is the atmospheric pressure (98.1 kPa). The parameter Q is an empirical constant, depending on the crushability features of sand: it increases with increasing resistance to crushing and, in particular, it is equal to 10 or more for silica sands. As carbonate sands are crushable, we can expect Q to be smaller for these soils. Values of Q equal to 7.5, 8.5 and 10.8 were assumed in Eq.(13) for Quiou, Kenya and Ticino rsands, as suggested by Randolph et al. [88] for these sands.

CRR-ξ_R data points for Ticino silica sand (Fig.15) are compared with the field-based relationship proposed for silica sands by Idriss [89]. The cyclic strength is referred to the cyclic resistance ratio at 15 cycles of loading in simple shear tests (CRR_{15}). Consistently with the correlation between state parameter and soil dilatancy, the data show that CRR_{15} increases as ξ_R becomes more negative. In particular, the laboratory data points were found to be in good agreement with the published field-performance correlation. The

experimental data for the (non-skeletal) carbonate Kenya sand fall close to the field-based relationship proposed for silica sands as well. On the other hand, *CRR*-ξ_R laboratory-based data points for the (skeletal) carbonate Quiou sand lie slightly above the curve suggested in the literature for silica sands. It means that, at a given value of ξ_R, the undrained cyclic resistance of carbonate sands is higher (or at least comparable) with respect to silica sands, as already discussed in the section 3.2.

It is worthwhile noticing that the relationship between cyclic strength and ξ_R offers the advantage that the effects of confining stresses on *CRR* (i.e., the K_σ effect) are included in the *CRR*-ξ_R correlation (Fig.15).

6. Conclusive remarks

In this study, a comprehensive investigation including a series of constant volume cyclic simple shear tests and bender element tests in triaxial cell was performed on three carbonate sands of different origin (Quiou, Dubai, Kenya) with the intent of assessing liquefaction resistance from shear wave velocity. For the sake of comparison, two silica sands having grain size features and initial state conditions (before shearing) similar to the carbonate sands were also tested.

The main findings achieved are the following:

- Important differences between the undrained cyclic response of carbonate and silica sands tested under similar conditions were observed. In particular, carbonate sands developed: 1) higher excess pore pressure ratios with large fluctuations between loading cycles, and 2) higher (or at least comparable) liquefaction resistance with respect to silica sands at similar density state before shearing.
- The undrained cyclic behaviour of the oolitic (non-skeletal) Kenya sand was found to be to some extent more similar to a silica sand, consistently with previous findings reported in the literature from monotonic loading tests [9].
- As expected for silica sands, the undrained cyclic strength of Kenya sand in a dense state decreases as the effective vertical stress increases. On the other hand, loose specimens of Quiou sand manifested an opposite behaviour with increasing effective vertical stress.

  The increase of *CRR* with increasing σ'_{v0} appears the result of a complex phenomenon due to crushing effects (i.e. micro-crushing of the asperities and/or breakage of the grains), and it could be a function of several factors such as:

hardness, shape, and internal porosity of grains. This “unusual” behaviour exhibited by Quiou sand was observed also by other authors in undrained cyclic triaxial and simple shear tests for various crushable soils.

- Since the effective overburden stress and depth influence the measured undrained cyclic strength of carbonate sands, it is convenient to introduce a *CRR* stress normalization procedure, for which *CRR* at a given σ'_{v0} is normalized as a function of effective vertical stress through an empirical exponent, *n*. In this case, the results are well described by a unique *CRR-N* relationship, regardless of initial vertical effective stress. The application of the described normalization procedure to the tested sands together with additional selected literature data on carbonate sands, provides a wide range of the exponent ($0.44<n<1.28$) for effective overburden stress up to 600 kPa.
- The data points of the carbonate sands in the *CRR*-V_{S1} plot fall to the right of field-based relationships developed for clean silica sands [10, 79] and it mayn be primarily ascribed to the typically higher V_S values exhibited by these materials in comparison with silica sands at the same density state. The results suggest that the currently used *CRR*-V_S liquefaction boundary curves proposed for silica sands are not conservative when applied to carbonate crushable sands. These findings are in agreement with those recently reported in the literature on calcareous Cabo Rojo sand, tested in undrained cyclic simple shear apparatus [24].
- The CRR_{field} data points gathered from laboratory tests on Ticino (silica) and Quiou (carbonate) were also compared with field-based liquefaction boundary curves based on normalized cone resistance proposed in the literature for silica sands. Such a comparison reveals that the experimental data for Quiou sand lie on the left side of the corresponding field-based curves of silica sands which appear to provide a slightly conservative estimation of liquefaction resistance of calcareous sands. The opposite trend exhibited by calcareous sands against silica sands depending on whether their liquefaction susceptibility is evaluated by correlations with *CPT* or V_S finds an explanation by the fact that, at comparable values of void ratio and stress level, the penetration resistance in carbonate sands is lower than in silica sands, whereas the shear wave velocity is generally higher.
- A strong correlation exists between the cyclic strength of carbonate sands (Quiou, Kenya) and the relative state parameter (ξ_R) introduced by Boulanger [82] to

describe the combined effect of void ratio and consolidation stress. More specifically, the undrained cyclic strength decreases as ξ_R increases at a rate that progressively decreases. It was found that data points in the *CRR*-ξ_R plane lie close to (Kenya) or slightly above (Quiou) the curve suggested in the literature for clean silica sands confirming the general trend that, at a given value of ξ_R, *CRR* of carbonate sands is higher (or at least comparable) with respect to silica sands.

Lastly, the authors hope that more numerous laboratory test data (preferably from simple shear tests) are collected in the literature on other carbonate sands, in order to develop "soil-specific" reliable correlations for liquefaction evaluation of these soils.

References

[1] Brandes HG. Simple Shear Behavior of Calcareous and Quartz Sands. Geotechnical and Geological Engineering 2011;29(1):113-126. https://doi.org/10.1007/s10706-010-9357-x.

[2] Safinus S, Hossain MS, Randolph MF. Comparison of Stress-Strain Behaviour of Carbonate and Silicate Sediments. In: Proceedings of the 18th International Conference on Soil Mechanics and Geotechnical Engineering, Paris, September 2-6, 2013, Technical Committee 101, pp. 267-270.

[3] Al-Douri RH, Poulos HG. Static and Cyclic Direct Shear Tests on Carbonate Sands. Geotechnical Testing Journal 1991;15(2):138-157.

[4] Celestino TB, Mitchell JK. Behavior of carbonate sands for foundations of offshore structure. In: Proceedings, Brazil offshore ’83, Rio de Janeino;1983, pp. 85-102.

[5] Coop MR, Airey DW. Carbonate sands. In: Characterizations and engineering properties of Natural soils, (Than et al., ed.), Swets and Zeitlinger, Lisse; 2003, pp. 1049-1086.

[6] Datta M, Gulhati SK, Rao GV. Crushing of calcareous sands during shear. In: Proceedings, offshore technology conference, Houston; 1979, Vol. 3, pp. 1459-1467.

[7] Ong SE, Joer HA, Randolph MF. Frictional behavior in calcareous soils. In: Engineering for calcareous sediments, proceedings of the 2nd international conference on engineering for calcareous sediments, (K.A. Al-Shafei ed.), Bahrain; 1999, Vol 1, pp. 219-228.

[8] Semple RM. The mechanical properties of carbonate soils. In: Engineerings for calcareous sediments, proceedings of the international conference of calcareous sediments, (R.J. Jewell, m.s. Khorshid eds), Perth; 1988, Vol. 2, pp. 807-836.

[9] Golightly CR. Engineering properties of carbonate sands. PhD thesis, University of Bradford, USA; 1988.

[10] Andrus RD, Stokoe II KH. Liquefaction resistance of soils from shear wave velocity. J. Geotech. Geoenviron. Eng. 2000;126(11):1015-1025. https://doi.org/10.1061/(ASCE)1090-0241(2000)126:11(1015).

[11] Youd TL, Idriss IM, Andrus RD, Arango I, Castro G, Christian JT, Dobry R, Finn WDL,

Harder LF Jr, Hynes ME, Ishihara K, Koester JP, Liao SSC, Marcuson III WF, Martin GR, Mitchell JK, Moriwaki Y, Power MS, Robertson PK, Seed RB, Stokoe KH. Liquefaction resistance of soils: Summary Report from the 1996 NCEER and 1998 NCEER/NSF Workshops on Evaluation of Liquefaction Resistance of Soils. J. Geotech. Geoenviron. Eng. 2001;127(10):817-833. https://doi.org/10.1061/(ASCE)1090-0241(2001)127:10(817).

[12] Andrus RD, Stokoe II KH, Juang CH. Guide for Shear-Wave-Based Liquefaction Potential Evaluation. Earthquake Spectra 2004;20(2):285-308. https://doi.org/10.1193/1.1715106.

[13] Seed HB. Soil liquefaction and cyclic mobility evaluation for level ground during earthquakes. J. Geotech. Eng. Division 1979;105(2):201-255.

[14] Tokimatsu K, Uchida A. Correlation between liquefaction resistance and shear wave velocity. Soils and Foundations 1990;30(2):33-42. https://doi.org/10.3208/sandf1972.30.2_33.

[15] Chen TM, Zhou YG, Ke H. Shear wave velocity-based liquefaction resistance evaluation: semi-theoretical considerations and experimental validations. In: The 14 WCEE, Beijing, China; October 12-17, 2008.

[16] Roy B. Liquefaction susceptibility and shear wave velocity. In: Proceedings of the 16th International Conference on Soil Mechanics and Geotechnical Engineering-Geotechnology in Harmony with the Global Environment. Osaka, Millpress Science Publishers/IOS Press, ISBN 978-90-5966-027-4, Japan; September 12-16, 2005, pp. 435-438. 10.3233/978-1-61499-656-9-435.

[17] Chen Y, Ke H, Chen RP. Correlation of shear wave velocity with liquefaction resistance based on laboratory tests. Soil Dynamics and Earthquake Engineering, 2005;25:461–469. 10.1016/j.soildyn.2005.03.003.

[18] Zhou YG, Chen YM. Laboratory Investigation on Assessing Liquefaction Resistance of Sandy Soils by Shear Wave Velocity. J. Geotech. Geoenviron. Eng. 2007;133(8). https://doi.org/10.1061/(ASCE)1090-0241(2007)133:8(959).

[19] Askari F, Dabiri R, Shafiee A, Jafari MK. Liquefaction resistance of sand-silt mixtures using laboratory based shear wave velocity. International Journal of Civil Engineering, 2011;9(2):136-144.

[20] Baxter CDP, Bradshaw AS, Green RA, Wang J. Correlation between cyclic resistance and shear-wave velocity for Providence silts. J. Geotech. Geoenviron.l Eng. 2008;134(1). https://doi.org/10.1061/(ASCE)1090_0241(2008)134:1(37).

[21] Dabiri R, Askari F, Shafiee A, Jafari MK. Shear wave velocity-based liquefaction resistance of sand-silt mixtures: deterministic versus probabilistic approach. IJST, Transactions of Civil Engineering 2011;35(C2):199-215.

[22] Liu N, Mitchell LS. Influence of Nonplastic Fines on Shear Wave Velocity-Based Assessment of Liquefaction. J. Geotechn. Geoenviron. Eng. 2006;132(8):1091-1097. https://doi.org/10.1061/(ASCE)1090_0241(2006)132:8(1091).

[23] Dobling ML. Cyclic resistance-shear wave velocity relationships for Monterey and Cabo Rojo carbonate sand. Master's Theses, University of Rhode Island; 2013, pp. 153.

[24] Morales-Velez C, Baxter CDP, Pando MA. Evaluation of the Cyclic Resistance of an Uncemented Calcareous Sand Deposit from Puerto Rico Using Shear Wave Velocity. In: 6th Internatinal Conference on Earthquake Geotechnical Engineering, Christchurch, New Zealand; 1-4 November 2015.

[25] Pham HHG, Van Impe P, Van Impe W, Mengé P. Liquefaction assessment of crushable sands by shear wave velocity measurements. 15th FEA Research Symposium, ID 7161656, Ghent, Belgium; 2014. http://hdl.handle.net/1854/LU-7161656.

[26] Porcino D, Diano V. Shear Wave Velocity-Based Assessment of Liquefaction Resistance of Carbonate Sands. International Workshop on Metrology for Geotechnics. In: Proceedings of the 1st IMEKO TC4 International Workshop on Metrology for Geotechnics, P. Daponte, and A.L. Simonetti (Eds.), ISBN: 978-1-5108-4494-0, Benevento (Italy); 17-18 March 2016.

[27] ASTM D4253. Standard test methods for maximum index density and unit weight of soils using a vibratory table. ASTM international, West Conshohocken, PA; 2000, pp 1-14.

[28] ASTM D4254. Standard test methods for minimum index density and unit weight of and calculation of relative density. ASTM international, West Conshohocken, PA; 2000, pp 1-9.

[29] Bellotti R, Fretti C, Ghionna VN, Pedroni S. Compressibility and crushability of sands at high stresses. In: Proc. the First International Symposium on Calibration Chamber

Testing – SOCCT1, Potsdam, NY; 1991, pp. 79-90.

[30] Porcino D, Caridi G, Ghionna VN. Undrained monotonic and cyclic simple shear behaviour of carbonate sand. Géotechnique 2008;58(8):635-644.

[31] Porcino D, Ghionna VN, Zimmitti Z. Correlating in-situ test results for Dubai and Abu Dhabi biogenic calcareous sands. In: 15 th Pan-American Conference on Soil Mechanics and Geotechnical Engineering. p. 642-649, D. Manzanal and A.O. Sfriso (Eds.), ISBN: 978-1-61499-602-6, Buenos Aires, Argentina; 15-18 November 2015. 10.3233/978-1-61499-603-3-642.

[32] Lees A, Derek A, King SM. Cone penetrometer testing data from the carbonate sand fill. In: Proceedings of the Institution of Civil Engineers - Geotechnical Engineering, Palm Jumeirah, Dubai, 2013;166(3):253–267.

[33] Poulos HG, Bunce G. Foundation design for the Burj Dubai – The world's tallest building. In: 6th Internationale Conference on Case Histories in Geotechnical Engineering, Paper N. 147, Airlington, VA; August, 11-16, 2008.

[34] Fioravante V, Giretti D, Jamiolkovski M. Small strain stiffness of carbonate Kenya sand. Engineering and Geology 2016;161:65-80. http://dx.doi.org/10.1016/j.enggeo.2013.04.006.

[35] Van Impe PO, Wils L, Van Impe WF, Haegeman W. Laboratory testing issues related to crushable sands. In: Proceedings of the 18th International Conference on Soil Mechanics and Geotechnical Engineering, Paris; 2013, pp. 275-278.

[36] Porcino D, Caridi G, Malara M, Morabito E. An automated control system for undrained monotonic and cyclic simple shear tests. In: Proc. GeoCongress, ASCE, Edited by DeGroot et al., ISBN: 9780784408032, Atlanta, GA; 2006.

[37] Dyvik R, Berre T, Lacasse S, Raadim B. Comparison of truly undrained and constant volume direct simple shear tests. Géotechnique 1987;37(1):3-10.

[38] Finn WDL. Aspects of constant volume cyclic simple shear. In: Proc. Advances in the art of testing soils under cyclic conditions, ASCE Convention; 1985, pp. 74-98.

[39] Seed RB, Cetin KO, Moss RES, Kammerer AM, Wu J, Pestana JM, Riemer MF, Sancio RB, Bray RE, Kayen RE, Faris A. Recent advances in soil liquefaction engineering: a unified and consistent framework. In: 26th Annual ASCE Los Angeles Geotechnical

Spring Seminar, Keynote presentation, H.M.S. Queen Mary, Long Beach, California; 2003, pp. 1-71.

[40] Wu J, Kammarer AM, Riemer MF, Seed RB, Pestana JW. Laboratory study of liquefaction triggering criteria. In: 13th World Conference on Earthquake Engineering, Paper No. 2580, Vancuver, BC, Canada; 2004.

[41] Chen YM, Zhou YG. Technique standardization of bender elements and international parallel test. Geotech. Spec. Publ. 2006;150:90-97. https://doi.org/10.1061/40862(194)11.

[42] Jovicic V, Coop MR, Simic M. Objective criteria for determining Gmax from beneder element tests. Géotechnique 1996;42(2):357-362.

[43] Lee JS, Santamarina JC. Bender elements: Performance and signal interpretation. J. Geotech. Geoenviron. Eng. 2005;131(9):1063-1070. https://doi.org/10.1061/(ASCE)1090-0241(2005)131:9(1063) .

[44] Gu X, Yang J, Huang M, Gao G. Bender element tests in dry and saturated sand: Signal interpretation and result comparison. Soils and Foundations 2015;55(5):951-962. 10.1016/j.sandf.2015.09.002.

[45] Jafarian Y, Haddad A, Javdanian H Comparing the shear stiffness of calcareous sands under dynamic and cyclic straining. In: 7th International Conference on Seismology & Earthquake Engineering, paper 00723-LT, Iran (Tehran);18-21 May, 2015.

[46] Van Impe PO, Van Impe WF, Manzotti A, Menge P, Van den Broeck M, Vinck K. Compaction control and related stress-strain behaviour of off-shore land reclamations with calcareous sands. Soils and Foundations 2015;55(6):1474-1486. doi.org/10.1016/j.sandf.2015.10.012.

[47] Robertson PK. Comparing CPT and VS liquefaction triggering methods. J Geotechn. Geoenviron. Eng. 2015;141(9). https://doi.org/10.1061/(ASCE)GT.1943-5606.0001338.

[48] Schnaid F, Lehane BM, Fahey M. In situ test characterization of unusual soils. In: Proc. of ISC-2 on Geotech. Geophys. Site Characterization, 2004; pp. 49-74.

[49] Almeida MSS, Jamiolkowski M, Peterson RW. Preliminary results of CPT tests in calcareous Quiou sand. In: Proc. First International symposium on CC Testing, Postdam, NY; 1991, pp. 1-13.

[50] Baldi G, Bellotti R, Ghionna VN, Jamiolkowski M, Pasqualini E. Penetration resistance

and liquefaction of sands. In: Proc. XI ICSMFE, San Francisco, CA; 1985, pp.1-6.

[51] Porcino DD, Marciano' V. Evaluating liquefaction resistance of a calcareous sand using the cone penetration test. Paper No. 4.15a. In: (a cura di): Shamsher Prakash, Fifth Int. Conf. on "Recent Advances in Geotechnical Earthquake Engineering and Soil Dynamics and Symposium in Honor of Professor I.M. Idriss", Missouri University of Science and Technology, ISBN: 9781887009164, San Diego, California; May 24-29, 2010, pp. 1-9.

[52] Robertson PK, Wride CE. Cyclic liquefaction and its evaluation based on SPT and CPT. In: Final Contribution to the Proceedings of the 1996 NCEER Workshop on Evaluation of Liquefaction Resistance, Salt Lake City, Utah; 1997.

[53] Morioka BT, Nicholson PG. Evaluation of the liquefaction potential of calcareous sand. In: Proceedings of the Tenth International Offshore and Polar Engineering Conference, ISOPE-I-00-184, Seattle, Washington, USA; 28 May – 2 June, 2000.

[54] Ross MS, Nicholson PG. Liquefaction potential and cyclic loading response of calcareous soils. CE Research Report, University of Hawai, Manoa; 1995.

[55] Sandoval EA, Pando MA. Experimental assessment of the liquefaction resistance of calcareous biogeneous sands. Earth Sciences Research Journal, 2012;16(1):55-63.

[56] Elmamlouk H, Salem M, Agaiby SS. Liquefaction Susceptibility of Loose Calcareous Sand of Northern Coast in Egypt. In: Proceedings of the 18th International Conference on Soil Mechanism and Geotechnical Engineering, Paris; 2013.

[57] Hyodo M, Hyde AFL, Aramaki N. Liquefaction of crushable soils. Geotechnique, 1998;48(4):527-543. https://doi.org/10.1680/geot.1998.48.4.527.

[58] Kaggwa WS, Poulos HG. Comparison of the behaviour of dense carbonate sediments and silica sand in cyclic triaxial tests. Research report, University of Sidney; 1990.

[59] LaVielle TH. Liquefaction susceptibility of uncemented calcareous sands from Puerto Rico by cyclic triaxial testing. Master of Science thesis, University of Blacksburg, Virginia; 2008.

[60] Sharma SS, Ismail MA. Monotonic and Cyclic Behavior of Two Calcareous Soils of Different Origins. J Goetech. Geoenviron. Eng. 2006;132(12). https://doi.org/10.1061/(ASCE)1090-0241(2006)132:12(1581).

[61] Pando MA, Sandoval EA, Catano J. Liquefaction Susceptibility and Dynamic Properties of Calcareous Sands from Cabo Rojo, Puero Rico. In: 15 WCEE, ISBN: 978-1-63439-651-6, Lisboa, Portugal; 24-28 September 2012.

[62] Boulanger RW, Idriss IM. State normalization of penetration resistances and the effect of overburden stress on liquefaction resistance. In: Proc. 11th International Conf. on Soil Dynamics and Earthquake Engineering and 3rd International Conference on Earthquake Geotechnical Engineering, Univ. of California, Berkeley, CA; 2004, pp. 484-491.

[63] Hynes ME, Olsen RS. Influence of Confining Stress on Liquefaction Resistance. Proc., International Workshop on Phys., and Mech. of Soil Liquefaction, Balkema, Rotterdam, The Netherlands; 1999, pp. 145–152.

[64] Stedman JD. Effects of Confining Pressure and Static Shear on Liquefaction Resistance of Fraser River Sand. BASc Thesis, University of British Columbia, Canada; 1997.

[65] Giang HH, Van Impe PO, Van Impe WF. Effects of particle characteristics on the shear strength of calcareous sand. Acta Geotechnica Slovenica, 2017/2, pp.77-89 ISSN: 1854-0171.

[66] Aramaki N, Okabayashi T, Hyodo M. Liquefaction characteristics of crushable volcanic soil “Shirasy”. 4th International Conference on Earthquake Geotechnical Engineering, Paper No. 1288, Thessaloniki, Greece; June 25-28, 2007.

[67] Montgomery J, Boulanger RW, Harder LF Jr. Examination of the K_σ overburden correction factor on liquefaction resistance. Report No. Ucd/Cgm-12/02 Center for Geotechnical Modeling, Department of Civil And Environmental Engineering University of California Davis, California, December 2012.

[68] Idriss IM, Boulanger RW. Soil liquefaction during earthquakes. Monograph Mno-12, Earthquake Engineering Research Institute, Oakland, CA; 2008.

[69] Mirbaha K. Bi-directional Cyclic Behaviour and Liquefaction Analysis of a silica-carbonate sands. Eletronic Thesis and Dissertation Repository. 5035, University of Wester Ontario, 2017. https://ir.lib.uwo.ca/etd/5035.

[70] Porcino D, Caridi G. and Ghionna V.N. Drained and undrained monotonic behaviour of sand in simple shear tests. In: 11 th Int. onference on Computer Methods and Advances

in Geomechanics-Prediction, analysis and design in Geotechnical applications. vol. 2, p. 183-190, G. Barla and M. Barla (eds), ISBN: 9788855528122, Torino; 19-24 Jun 2005.

[71] Coop MR. The mechanics of uncemented carbonate sands. Géotechnique, 1990, 40(4), 607-626.

[72] Finnie IMS, Hospers B, Nowacki F, Andersen KH, Kalsnes B. Cyclic simple shear behaviour of carbonate sand. Engineering for Calcareous Sediments, Al-Shafei (ed.), Balkema, Rotterdam, ISNB 90 5809 037 X; 1999.

[73] Bhatia S, Schwab J, Ishibashi I. Cyclic simple shear, torsional shear and triaxial – A comparative study. In Advances in the art of testing soils under cyclic conditions, ASCE; 1985, pp. 232-254.

[74] Kammerer AM, Wu J, Riemer M, Pestana JM, Seed RB. Use of cyclic simple shear testing in evaluation of the deformation potential of liquefiable soils. Proc. of the Forth International Conference on Recent Advantaces in Geotechnical Earthquake Engineering and Soil Dynamic and Symposium in Honor of Professor W.D. Liam Finn, Paper No. 1.20, San Diego, California; 26-31 March, 2001.

[75] Mao X, Faher M. Behaviour of calcareous soils in undrained cyclic simple shear. Géotechnique, 2003;53(8):715-727. https://doi.org/10.1680/geot.2003.53.8.715.

[76] Wu J. Liquefaction triggering and post-liquefaction deformation on Monterey 0/30 sand under uni-directional cyclic simple shear loading. Ph. D. Thesis, University of California, Berkley; 2002.

[77] Porcino D, Saccenti A. Normalisation of cyclic undrained triaxial and simple shear strength of carbonate sand to monotonic shear strength. In: Proc. of International Conf. on Performance-Based Design in Earthquake Geotechnical Engineering. Japan, 15-18 June 2009, p. 1527-1534; 2009.

[78] Tatsuoka F, Ochi K, Fujii S, Okamoto M. Cyclic undrained triaxial and torsional shear strength of sands for different sample preparation methods. Soil and Foundations, 1986;26(3):23-41. https://doi.org/10.3208/sandf1972.26.3_23.

[79] Kayen R, Moss RES, Thompson EM, See RB, Cetin KO, Der Kiureghian A, Tanaka Y, Tokimatsu K. Shear-wave velocity-based probabilistic and deterministic assessment of seismic soil liquefaction potential. J. Geotech. Geoenviron. Eng. 2013;139(3):407-419.

https://doi.org/10.1061/(ASCE)GT.1943-5606.0000743.

[80] Liu AH, Stewart JP, Abrahamson NA, Morikawi Y. Equivalent number of uniform stress cycles for soil liquefaction analysis. J. Geotech. Geoenviron. Eng. 2001;127(12):1017-1026. https://doi.org/10.1061/(ASCE)1090-0241(2001)127:12(1017).

[81] Kayen R, Seed RB, Moss RE, Cetin KO, Tanaka Y, Tokimatsu K. Global shear wave velocity database for probabilistic assessment of the initiation of seismic-soil liquefaction. In: 11th International Conference on Soil Dynamics and Earthquake Engineering, Berkeley, CA; January 7-9, 2004.

[82] Boulanger RW. Evaluating Liquefaction Resistance at High Overburden Stresses. Proc. Third US-Japan Workshop on Advanced Research on Earthquake Engineering for Dams, Sand Diego, CA; 2002, pp. 22-23.

[83] Idriss IM, Boulanger RW. Semi-empirical procedures for evaluating liquefaction potential during earthquakes. Soil Dynamics and Earthquake Engineering 2006;26:115-130. 10.1016/j.soildyn.2004.11.023.

[84] NCEER. Proc. the NCEER Workshop on Evaluation of the Liquefaction Resistance of Soils, Salt Lake City, Utah, Technical Report NCEER-97-022; 1997.

[85] Coop MR. On the mechanics of reconstituted and natural sands. Deformation Characteristics of Geomaterials, Recent Investigation and Prospects (Di Benedetto et al., ed.), Taylor and Francis Group, London; 2005, pp.29-58.

[86] Boulanger RW. High overburden stress effects in liquefaction analyses. Journal Geotechnical and Geoenviromental Engineering, 2003;129(12):1071-1082. https://doi.org/10.1061/(ASCE)1090-0241(2003)129:12(1071).

[87] Bolton MD. The strength and dilatancy of sands. Géotechnique, 1986;36(1):65-78. https://doi.org/10.1680/geot.1986.36.1.65.

[88] Randolph MF, Jamiolkowski MB, Zdravkovic L. Load carrying capacity of foundations. Proc. Advances in Geotechnical Engineering: The Skempton Memorial Conference, London, U.K.; 2004, Vol. 1, pp. 207-240.

[89] Idriss IM. An update to the Seed-Idriss simplified procedure for evaluating liquefaction potential. TRB Workshop of New Approches to Liquefaction, Publication No. FHWARD-99-165, Federal Highway Administation; 1999.

Table 1

Physical and mineralogical properties of tested sands.

Sand	Kenya (*KS*) Carbonate non skeletal	Dubai (*DS*) Carbonate skeletal	Quiou (*QS*) Carbonate skeletal	Ticino (*TS*) silica	Ticino fine (*TSF*) silica
D_{50} [mm]	0.13	0.17	0.68	0.55	0.18
U_c	1.86	2.46	5.04	1.60	1.91
e_{max}	1.776	1.118	1.282	0.927	0.978
e_{min}	1.282	0.573	0.833	0.578	0.613
G_s	2.780	2.690	2.702	2.681	2.690
$CaCo_3$ [%]	92	55	75	0	0

Note: e_{max} and e_{min} were determined using ASTM D4253 [27] and ASTM D4254 [28] procedures.

Table 2

Test summary program.

Sand	Test type	I_r (%)	p'_0 (kPa)	σ'_{v0} (kPa)	Reconstitution method
Kenya	*BE – CSS*	69	25 – 250	50 – 200	Air Pluviation (*AP*)
Dubai	*BE – CSS*	75	25 – 150	100	Air Pluviation (*AP*)
Quiou	*BE – CSS – CTX*	20 – 80	25 – 250	100 – 200	Water Sedimentation (*WS*)
Ticino	*BE – CSS*	30 – 80	10 – 450	100	Water Sedimentation (*WS*) Air Pluviation (*AP*)
Ticino fine	*BE – CSS*	62	25 – 300	100	Air Pluviation (*AP*)

BE = bender elements in triaxial cell

CSS = undrained cyclic simple shear

CTX = undrained cyclic triaxial test

I_r = density index at the end of consolidation phase

p'_0 = mean effective consolidation stress in triaxial cell

σ'_{v0} = effective vertical consolidation stress in simple shear apparatus

Table 3

Values of the empirical parameters of Eq.(3).

Material	Test type	Reconstitution Method	σ'_{v0} (kPa)	I_r (%)	A	B	R^2
Kenya	*CSS*	*AP*	50	69	0.313	0.194	0.91
Kenya	*CSS*	*AP*	100	69	0.298	0.233	0.93
Kenya	*CSS*	*AP*	200	69	0.261	0.245	0.99
Quiou	*CSS*	*WS*	100	45	0.250	0.201	0.99
Quiou	*CSS*	*WS*	200	45	0.269	0.195	0.95
Quiou	*CSS*	*WS*	100	75	0.477	0.291	0.84
Quiou	*CTX*	*WS*	100	45	0.455	0.199	0.99
Quiou	*CTX*	*WS*	100	75	0.544	0.191	0.97
Ticino fine	*CSS*	*AP*	100	62	0.215	0.175	0.98
Ticino	*CSS*	*AP*	100	45	0.189	0.182	0.95
Ticino	*CSS*	*AP*	100	80	0.283	0.226	0.98
Ticino	*CSS*	*WS*	100	45	0.292	0.272	0.96

Table 4

Values of the empirical parameter n (Eq.5) calculated for different crushable materials.

Material	Mineralogy	Gradation and particle shape	Type test	I_r (%)	σ'_{v0} (kPa)	p'_0 (kPa)	n	Reference
Quiou	Biogenic carbonate sand	*WG*, *SA*	*CSS*	45	200	-	1.13	Present study
Kenya	Oolitic carbonate sand	*PG*, *SR*	*CSS*	69	50 - 200	-	0.78	Present study
North Coast	Biogenic carbonate sand	*PG*, *SA to A*	*CTX*	40	-	50 - 200	0.57	Elmamlouk et al. [56]
Cabo Rojo	Biogenic carbonate sand	*PG*, *SA* to *A*	*CTX*	45 - 50 65 80	-	200	0.77 0.44 0.44	Pando et al. [61]
Dogs Bay	Biogenic carbonate sand	*PG*, *HA* and *P*	*CTX*	60 80	-	300 - 500	1.04 0.79	Hyodo et al. [57]
Boler	Carbonate-silica sand	*PG*, *SA* to *A*	*CSS*	45 65	50 - 600	-	1.24 1.28	Mirbaha [69]

* *SA*= Sub Angular; *A*= Angular; *SR*= Sub Rounded; *HA*= Highly Angular; *P*= Platey; *WG*= Well-graded; *PG*= Poorly-graded.

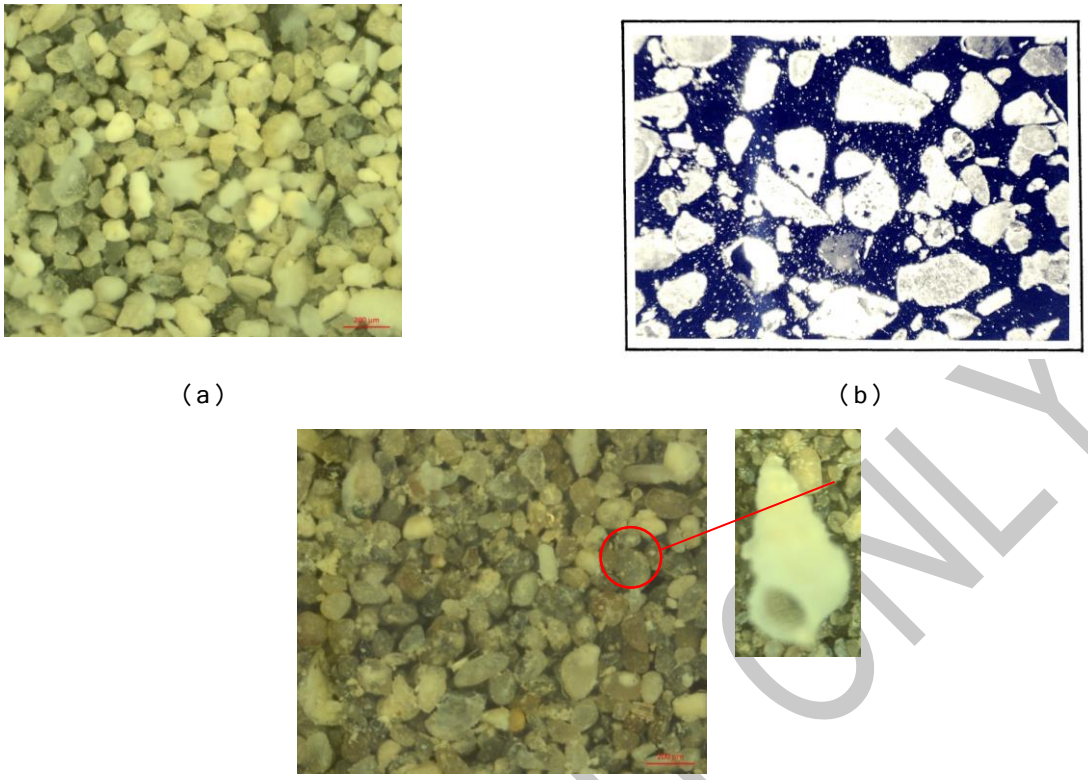

Fig.1. Micrographs of the calcareous sands tested in the present study: (a) Kenya, (b) Quiou and (c) Dubai.

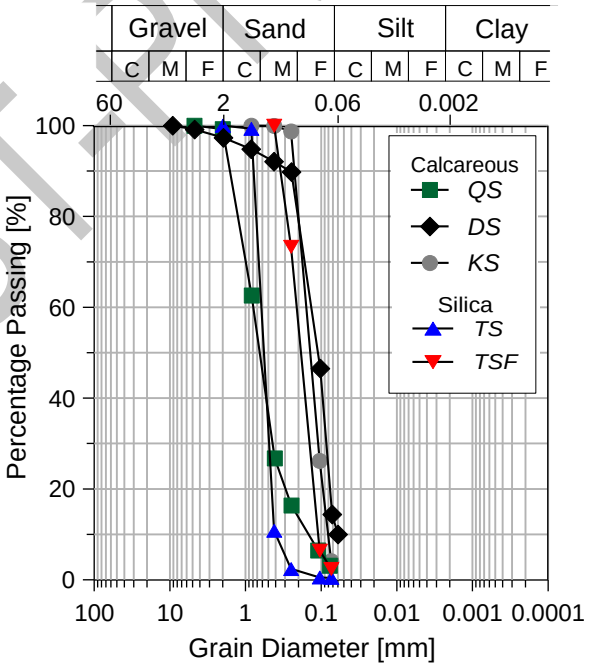

Fig.2. Grain size distribution curves of the tested materials.

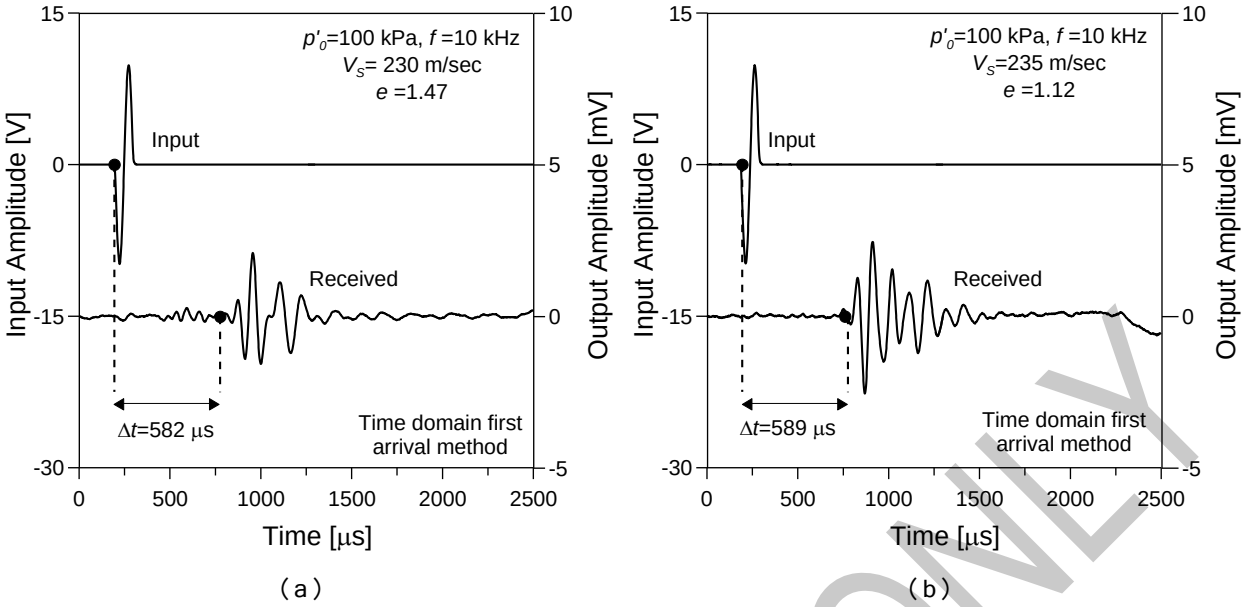

Fig. 3. Typical records of bender element tests on carbonate sands: (a) Quiou and (b) Kenya.

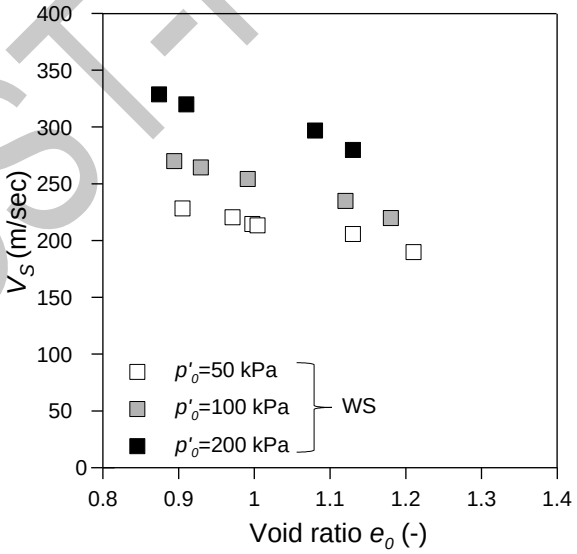

Fig. 4. Influence of void ratio and effective confining stress on V_S of carbonate Quiou sand.

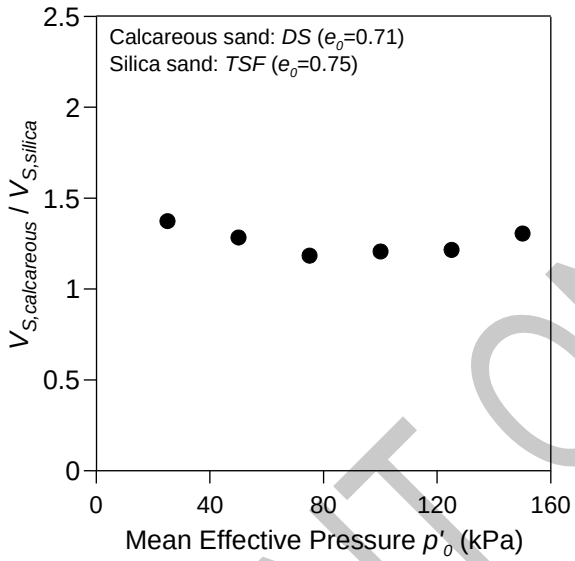

Fig. 5. Comparison between V_S measurements on silica and calacareous sands tested at similar void ratios.

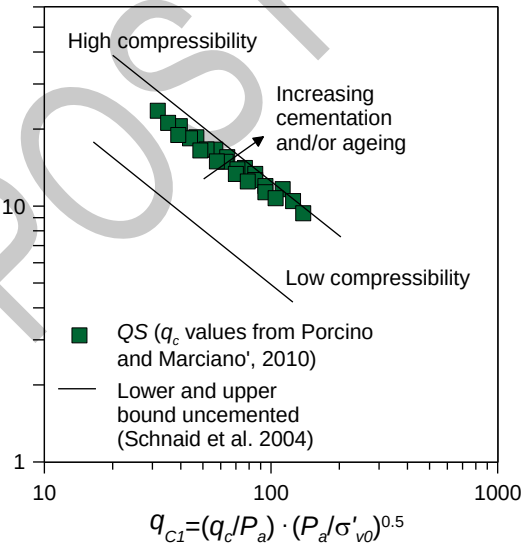

Fig. 6. Correlation between G_0 (*BE*) and q_c (*CC*) for Quiou calcareous sand.

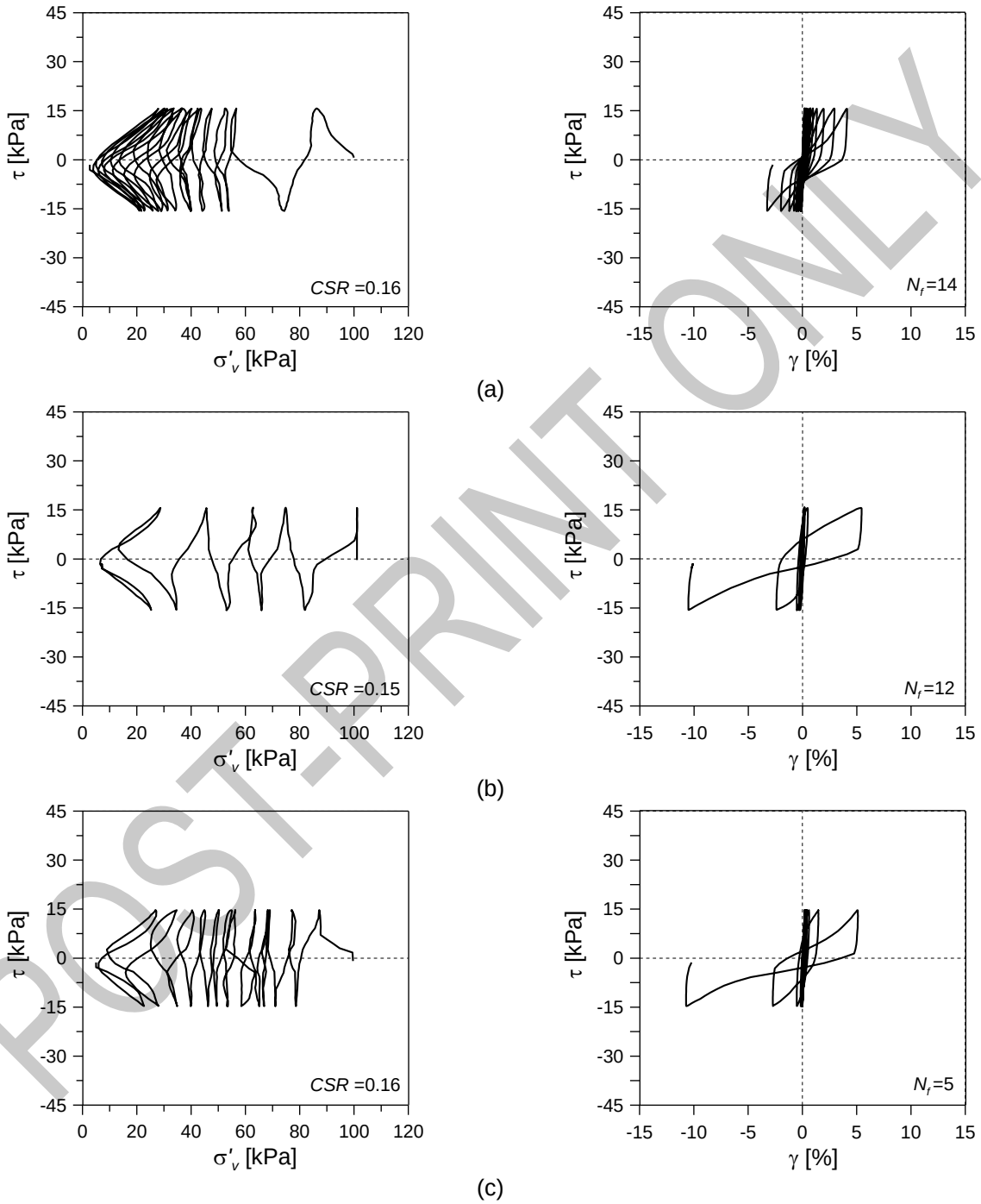

Fig. 7. Comparative cyclic *SS* test results performed on (a) Dubai carbonate sand, (b) Kenya carbonate sand (c) Ticino fine silica sand (All tests: air-pluviated, medium dense specimens, σ'_{v0}=100 kPa).

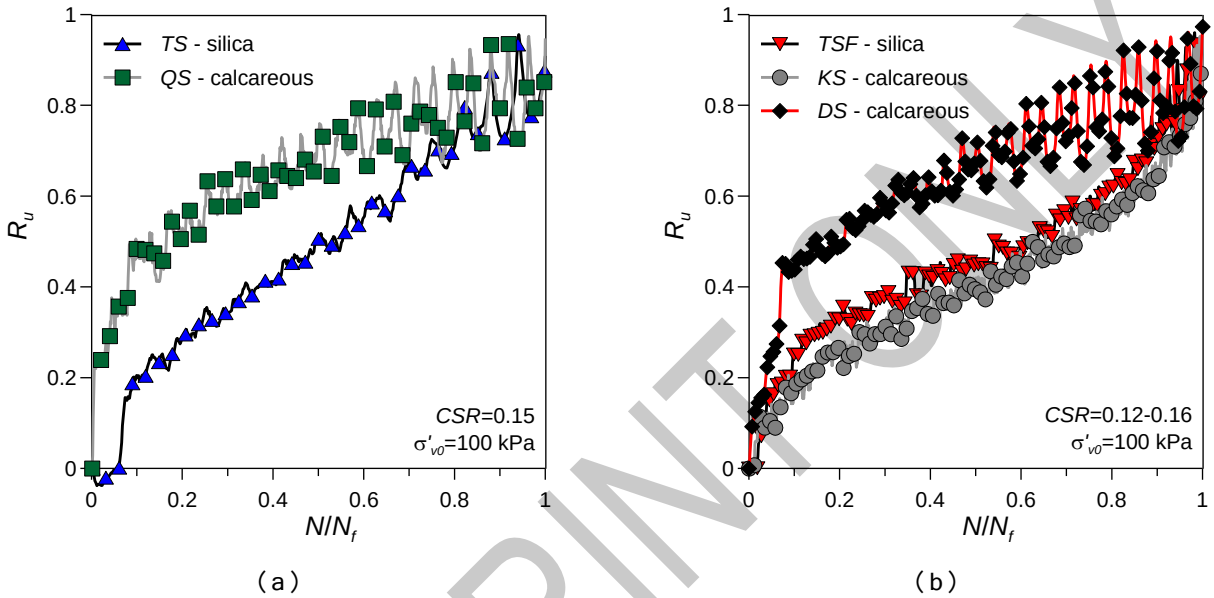

Fig.8. Influence of mineralogical features on excess pore water pressure generation curves of: (a) loose sand specimens and (b) medium dense to dense sand specimens.

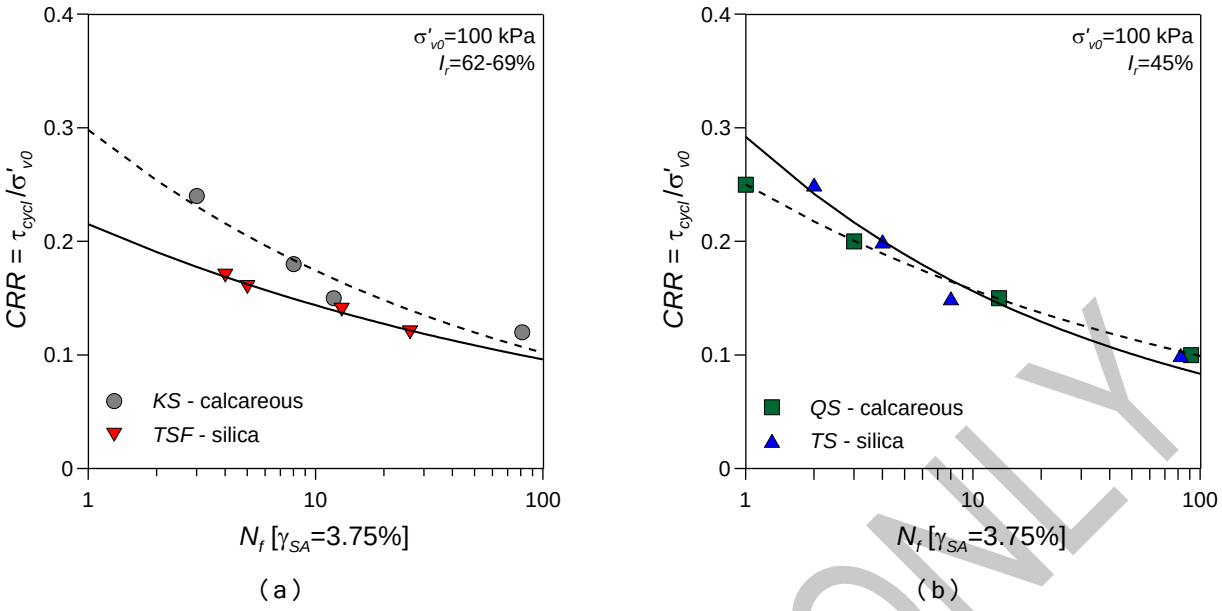

Fig.9. Cyclic resistance curves for calcareous vs. silica sands.

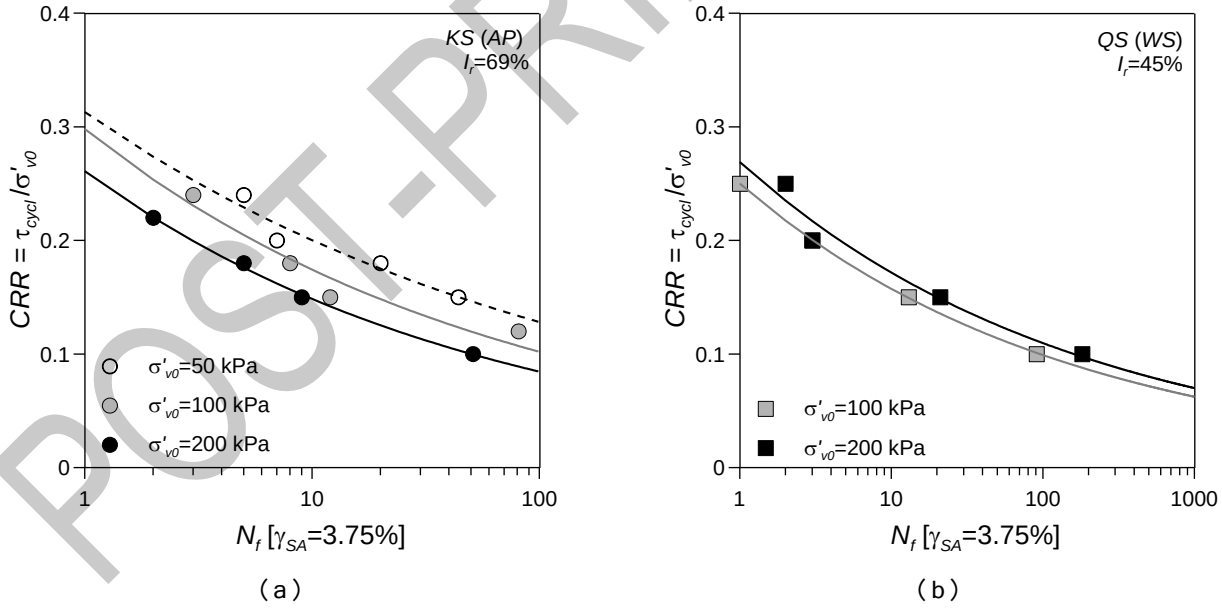

Fig.10. Effect of initial effective vertical stress on cyclic shear strength of two calcareous sands (a) Kenya sand, air pluviated, medium dense and (b) Quiou sand, water pluviated, loose.

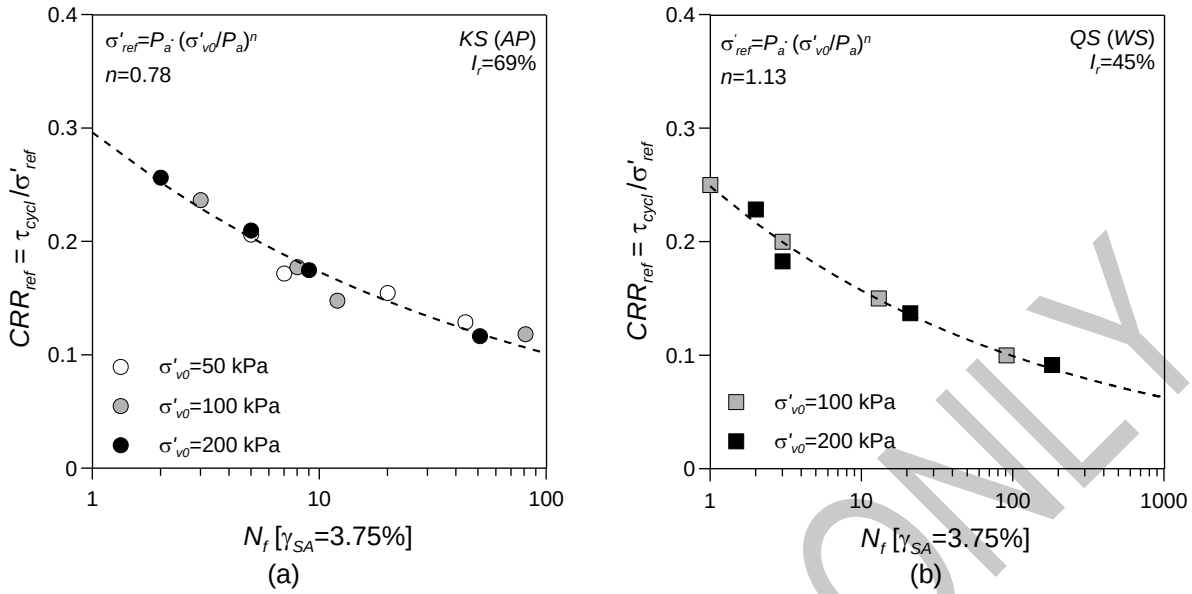

Fig. 11. Cyclic resistance curves normalized to s'ref according to Eq.(5): (a) Kenya sand, medium dense and (b) Quiou sand, loose.

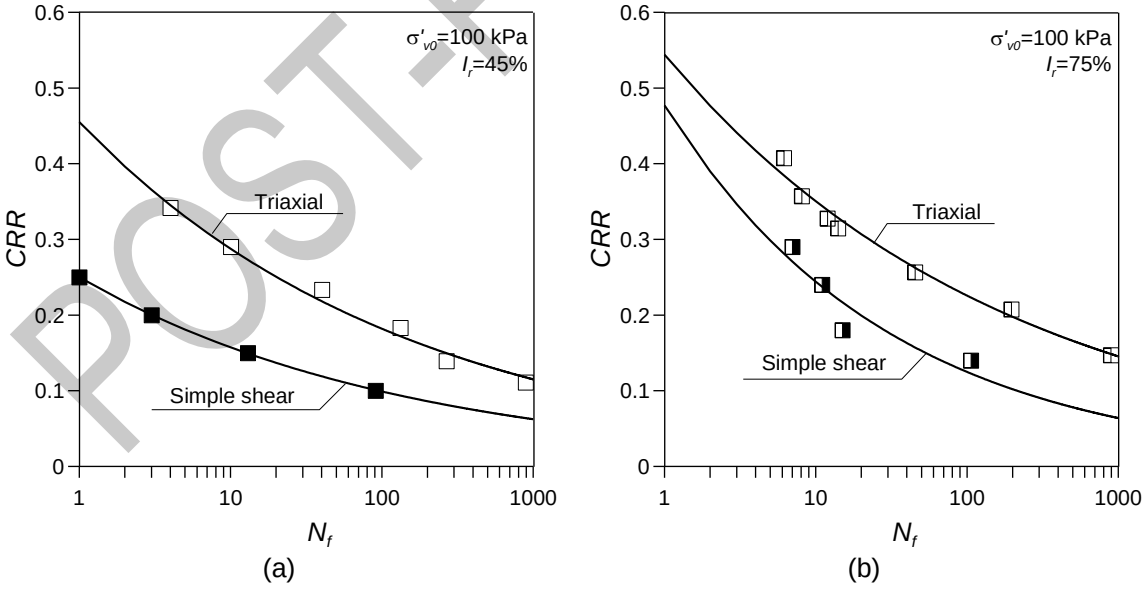

Fig. 12. Effect of loading mode on cyclic shear strength of Quiou calcareous sand (a) loose and (b) dense specimens.

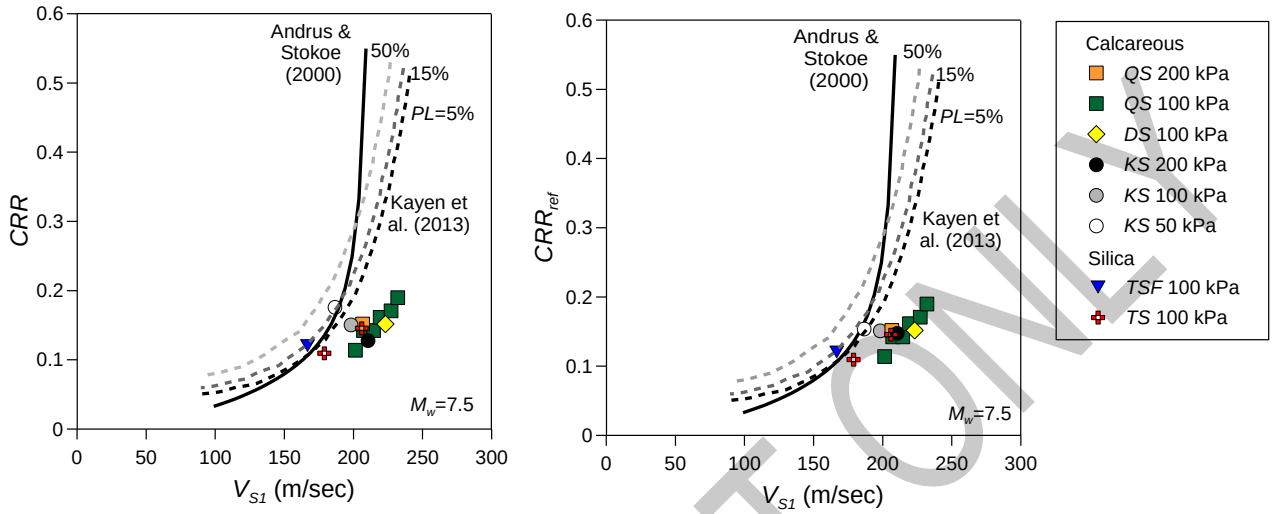

Fig. 13. Correlation between CRR_{field} and V_{S1} for carbonate sands and comparison with predicted trends for silica sands (a) before and (b) after stress-normalization of *CRR* values according to Eq.(4).

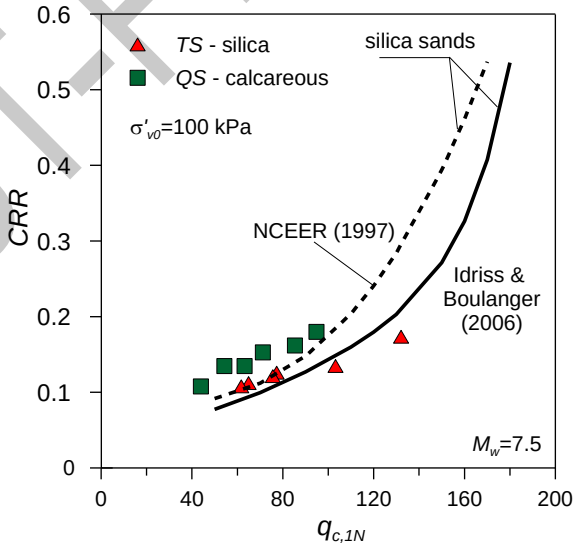

Fig. 14. *CRR* vs $q_{c,1N}$ correlation gathered for Quiou carbonate sand and comparison with the trends proposed in the literature for silica sands.

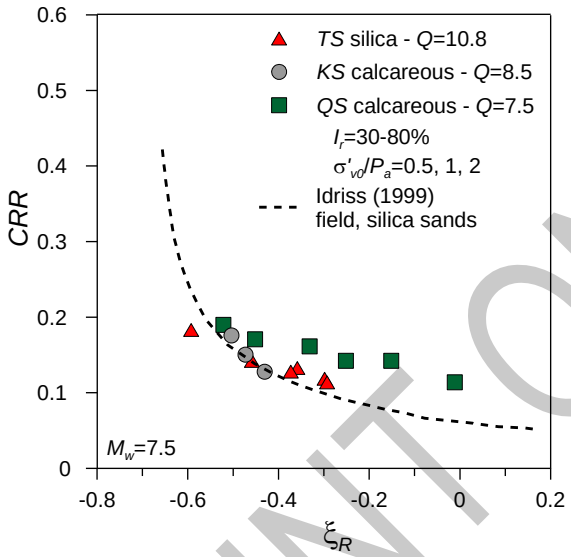

Fig. 15. *CRR* vs. relative state parameter (ξ_R) correlation gathered for Quiou and Kenya carbonate sands and comparison with the trend proposed in the literature for silica sands.